Reassessing Electrothermal Simulation Techniques to Develop Realistic Models

T. Lijnse[1*], S. Cenaiko[2], G. Moscoso[3], C. Dalton[1,4]

1. Biomedical Engineering Graduate Program, University of Calgary, Calgary, AB, Canada
2. Chemical and Petroleum Engineering, University of Calgary, Calgary, AB, Canada
3. Mechanical and Manufacturing Engineering, University of Calgary, Calgary, AB, Canada
4. Electrical and Computer Engineering, University of Calgary, Calgary, AB, Canada

* thomas.lijnse@ucalgary.ca

Abstract: Electrokinetic (EK) techniques have been broadly implemented in a variety of fields, including microfluidics and lab-on-a-chip, and are seeing increased interest to miniaturize and optimize fluid pumping and mixing systems. While EK techniques such as electro-osmosis and dielectrophoresis have been implemented in limited application areas, particle sorting, and fluid mixing, AC Electrothermal (ACET) is a technique that has seen adoption in microfluidic pumping systems with high conductivity (> 0.2 S/m) fluids, such as biofluids and pharmaceuticals [1]. ACET pumping is well suited to high conductivity fluids as Joule heating is the primary driving force, which is directly proportional to fluid conductivity [2]. COMSOL is traditionally used as a modelling tool for ACET phenomena, due to the Multiphysics nature of the systems, incorporating AC/DC, heat transfer, and fluid flow modules. Most reported simulations in this area typically rely on 2D simulations, effective DC voltages, planar electrodes, and bypass channel wall behaviours to simplify the system to save on computational resources. This work addresses many of these factors and their individual and collective impacts on ACET modelling and flow rate accuracy. Our work shows significant discrepancies between flow rates under the simplification assumptions and our proposed, more realistic, model. Using modern enhanced computing tools, the results outlined in this work will allow for ACET and broader EK modelling to more closely resemble real devices and improve simulation accuracy to produce more meaningful theoretical results. This allows for model analysis and improvement with increased certainty that simulation changes reflect manufactured system outcomes. This will lead to better understanding and uptake of the technique.

Keywords: AC Electrothermal, microfluidics, Electrokinetics, microfabrication

Introduction

Lab-on-a-chip (LOC) systems are becoming increasingly commonplace in research, and increasingly complex. As these systems aim to integrate several complex reactions and analyses, the number of microfluidic channels and device inputs increases. Traditional syringe pumps used in microfluidic pumping are large and do not fit an end goal of miniaturized bedside technologies. To this end, electrokinetic (EK) methods, by which electric fields are applied to manipulate fluids and particulate, are an ideal candidate to handle increasing design complexity without sacrificing system size or reliability. This is due to advancements in fabrication methods allowing for the creation of intricate electrical and control systems in extremely small areas.

Alternating Current Electrothermal (ACET) systems are a type of EK system that uses applied electric fields in a conductive solution to generate Joule Heating. When the electric fields are applied asymmetrically, this causes a temperature gradient that drives fluid flow and mixing in microchannels. A typical ACET device configuration is seen in figure 1. This method has received attention in several fields, including microchip manufacturing [3], biological testing systems, and point of care medicine, [3]–[6]. This is due to its ability to manipulate fluids at relatively high velocities while requiring low operating voltages (< 10V), which will not damage channel media and integrates easily into pre-existing control systems.

The ACET effect is usually modelled in Multiphysics simulation software using a wide variety of geometries, boundary conditions, and analytical models due to the extreme complexity of the theory. Most simulations rely on a simplification to a 2D geometry, DC steady state equivalencies to applied AC signals, and other geometry and boundary

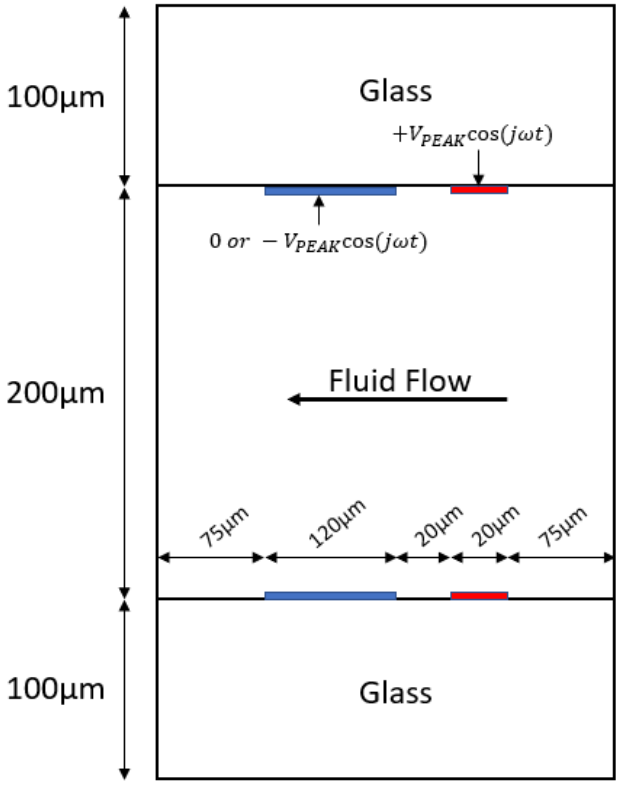

Figure 1: Layout of a typical ACET system, with electrodes patterned on both the top and bottom substrate. The red electrode is the signal to which the major driving signal is applied. The blue electrode is typically held at ground, or in opposition to the signal electrode in the case of 'travelling-wave' based systems. Dimensions given are from previous studies optimizing geometries [8].

simplifications to limit complexity and save computational resources [2], [7]–[9]. This work addresses the simplifications currently used, their individual impacts on system flow rates, and an analysis of their combined impact to determine overall model accuracy compared to real fabricated ACET systems. By developing models that better reflect real systems, research methods and ACET development can be improved, leading to better, more reliable EK based LOC systems on the market.

AC Electrothermal Systems

The ACET effect has been well established [2], [10], [11]. To implement ACET systems, variable width electrodes are patterned in a microchannel in a pair, one wide and one thin. When an alternating potential is applied to the thin electrode and the wide electrode is grounded an electric field gradient is established. In a sufficiently conductive solution (>0.2 S/m), such as most biofluids like blood or saliva, the energy balance in the system is between the electric field and the temperature gradient established through Joule heating seen in equation 1.

$$k\nabla^2 T + \sigma E^2 = 0 \tag{1}$$

Where k is the thermal conductivity of the fluid in W/m*K, σ is the electrical conductivity of the channel medium in S/m, E is the electric field V/m, and $\nabla^2 T$ is the thermal gradient in K. Given that in microsystems devices, lengths and widths establish charge movement as the major force over convective, buoyant, or gravitational forces, equation 2 is established from the analysis of coulombic and dielectric forces.

$$\langle f_e \rangle = \frac{1}{2} Re\left[\frac{(\sigma\nabla\epsilon - \epsilon\nabla\sigma)\cdot E}{\sigma + j\omega\epsilon}\cdot E^* - \frac{1}{2}|E|^2\nabla\epsilon\right] \tag{2}$$

Where ω is the applied signal angular frequency and ϵ is the media dielectric permittivity. Equation 2 establishes the relationship between the applied electric field and the electrical force on the body of the solution. The gradient of electrical conductivity and dielectric permittivity can both be related to the temperature gradient, as these values will change with a changing temperature. This yields equation 3, which establishes the relationship between a temperature gradient and the forces experienced in the channel.

$$\langle f_e \rangle = \frac{1}{2} Re\left[\frac{\sigma\epsilon(\alpha - \beta)}{\sigma + j\omega\epsilon}(\nabla T \cdot E)E^* - \frac{1}{2}\epsilon\alpha|E|^2\nabla \mathrm{T}\right] \tag{3}$$

Where alpha and beta are, respectively, $\left(\frac{1}{\epsilon}\right)\left(\frac{\delta\epsilon}{\delta T}\right)$ and $\left(\frac{1}{\sigma}\right)\left(\frac{\delta\sigma}{\delta T}\right)$ which are typically -0.4%K^{-1} and 2%K^{-1} for an aqueous solution. In a microchannel flow is typically laminar, where Re << 1 due to the extremely small dimensions. Due to this, the flow equation is established as seen in equation 4.

$$\eta\nabla^2 \upsilon - \nabla p + f_e = 0 \tag{4}$$

Where η is the fluid viscosity, υ is the fluid velocity, and p is the channel pressure. As the pressure differential from inlet to outlet in a microchannel is very small and the dominant geometry term is the channel length this can be approximately simplified to equation 5.

$$|\upsilon| = \langle F_E \rangle \cdot \frac{l^2}{\eta} \tag{5}$$

Eqns 1, 3, and 5, establish the primary links between the applied electric field, temperature gradient, and the electric and thermal forces on the fluid body. These equations create the basis for Multiphysics simulations modelling the electrothermal system.

Multiphysics Simulations

This work uses the electric currents module from the AC/DC systems, laminar flow from Fluid Flow, and heat transfer in solids from Heat Transfer. The combination of these three systems, including custom written equations, can incorporate all necessary physics equations previously discussed. Results are analyzed using custom equations representing Joule Heating derived from equation 1, as well as the Joule Heating Multiphysics module, implemented through the electromagnetic heating (EMH) module. As studies regarding EK systems are concerned with steady state flow, time averaged versions of the formulas are typically used. Time dependent studies were investigated, but due to the applied signal frequency and the time it takes for fluid flow to establish, COMSOL will not create a convergent solution. Several studies, both stationary and frequency-stationary are used to assess fluid flow. Mesh size is set to extra-fine unless otherwise specified. The channel is constructed as in figure 1 using a series of electrodes on the top and bottom of the channel, as has been demonstrated previously [12].

When not using the EMH module, joule heating is modelled through setting a fluid Heat Source where heating is equivalent to the thermal component in equation 1. ACET force on the fluid is implemented using equation 3 assigned as a Volume Force broken into the respective cartesian components.

Boundary conditions for fluid flow include zero pressure constraint at the inlet, as pressure will be generated in immediate vicinity to the electrodes, zero initial velocity and pressure, and a no-slip condition at the walls. At the macroscale, no-slip conditions are considered necessary, but this is not necessarily true with microscale electrokinetic devices, particularly due to the presence of an electric double layer [13]. There is, however significant evidence limiting the slip velocity in an electrokinetic system to the Helmholtz-Smoluchowski velocity, given by equation 6 [14].

$$u_{HS} = -\frac{\zeta\epsilon}{\mu_F} E_{||} \tag{6}$$

Where ζ is the zeta potential of the double layer and μ_F is the fluid viscosity in Pa*s. Zeta potential in ACET systems is very low, near negligible, as they use a high frequency which does not allow for the establishing of a double layer [15]. Additionally, the electric field is relatively small compared to traditional electroosmotic techniques, as in ACET voltages are on the order of ten volts rather than the kilovolt range. This puts the magnitude of any slip velocity in a negligible range.

Periodic conditions are applied to the channel inlet and outlet to mimic repeating units of electrodes. For heat transfer, the external boundaries of the channel walls are set to be standard room temperature (293.15 K). There are periodic conditions for

heat transfer for each channel wall and the fluid, and heat is allowed to freely conduct across all boundaries using the appropriate material densities and heat capacities. The heat convection model is changed as appropriate.

In the electric currents model, current conservation is set for the channel medium, electric insulation is applied to each of the channel walls, as these are typically made of glass, non-conductive polymers, or undoped silicon [2]. Periodic conditions are set for the inlet and outlet. The electrical conductivity conduction model is used, and the dielectric model is changed as necessary for the simulations, but is set to relative permittivity for the fluid.

Previous work has demonstrated applicability of dielectric coatings to improve ACET device performance [6], [16], and this work addresses several methods of dielectric coating and heating implementation. To improve simulation of flow specifically around the microelectrodes, we analyzed protrusion of electrodes into the channel, traditionally assumed to be of negligible height compared to the channel height and simulated as planar electrical sources[2]. Methods of analyzing time varying signals to equivalent time averaged DC signals are compared.

Heat transfer settings regarding convective flow cooling, thought to have negligible impact on flow rates, were also assessed [11]. Finally, the impacts of using a three-dimensional model, with no-slip and heat conduction at the sidewalls, was addressed.

Analysis

A baseline model was created using a two-dimensional simplification, assuming planar electrodes, a DC voltage approximation of the AC signal set at 4.95 V_{RMS} (7 V_{PEAK}), a frequency of 100 kHz and a fluid conductivity of 0.224 S/m. This model was selected as the baseline due to it being a common method of simulating ACET systems [2], [4], [9], [16]. While the applied signal is on the high end of simulation voltages, it allows for distinct variation in flow rates to better analyze unique effects. Measurements are a line average of outlet velocity parallel to the channel wall, referred to here as the 'x' component. Tangential components of the velocity, 'y', are not included in the summary as these are typically several orders of magnitude lower than the 'x' component.

Table 1: Summary of some changes addressed through simulation settings. Values compared to a reference flow rate of $9.42*10^{-5}$ m/s using the model from Figure 1.

Change	Output Flow Value	% error introduced
Exponential form applied signal	9.42E-05	0.00%
EMH module in place of heat source. Freq-Stationary Study	4.71E-05	-50.00%
EMH module in place of heat source. Stationary Study	9.42E-05	0.00%
Protrusion of electrodes into the channel (120nm)	1.03E-04	9.36%
Heat convection from velocity field	9.15E-05	-2.85%
Electrodes fixed at 293.15 K	5.42E-05	-42.47%
Temperature dependent viscosity	1.08E-04	14.4%

From these results we see that several fundamental changes to simulation parameters can have significant impacts on channel flow outcomes. Initially we can see that the implementation of a sinusoidal form of the applied signal voltage, of the form seen in equation 7, has a small impact when considering the 100kHz signal. A frequency-stationary study is used to address these impacts.

$$V = V_{PEAK} e^{j\omega t} \tag{7}$$

Measuring the impacts of the frequency dependent term across a broad frequency band yields no changes. This would imply that there is no relationship between frequency and flow rate, which we know to be false [17]. As previously addressed, time based simulations in COMSOL for high frequency analysis are not feasible, and as such COMSOL does not presently have the capabilities to accurately model frequency dependent changes in ACET flow.

The EMH addition to the system creates a significant flow discrepancy based on study settings. This is a key factor for electrokinetic systems, and particularly ACET systems. In a time stationary format, Joule Heating effects from the EMH module are assumed to be due exclusively to the heating term seen in equation 3. In a frequency analysis system, Joule Heating is split between the electric and magnetic heating terms as seen in equation 8.

$$Q_e = \frac{1}{2} Re(J \cdot E^*) + \frac{1}{2} Re(j\omega B \cdot H^*) \tag{8}$$

AC electrokinetics are primarily considered to be a quasi-electrostatic system in which the effects of magnetic fields are not considered. As such, the effective heating, and thus, flow rate, are halved. For accuracy in electrokinetic modelling, any heating effects must not incorporate a magnetic field component. Previous work has shown that extremely large magnetic fields must be applied to microfluidic systems in order to see impacts, which is not possible using low voltages [18].

Heat convection was determined to have a significant impact on channel flowrate. Previous analytical solutions to electrokinetic effects stated that convective flow is negligible [11], [15]. However, as ACET systems undergo several improvements to flow rate efficacy, the velocity terms which were previously of small enough magnitude to be excluded can no longer be ignored. As flow rates improve, the convective cooling factor will become more significantly detrimental and must be accounted for. Additionally, as heating is a major component, temperature at the electrode-electrolyte interface must be considered. The temperature in ACET systems has shown to be maximized a short distance above the electrode surface, but the electrodes themselves are at a fairly similar temperature due to their proximity, 299.08 K vs 298.60 K in the case of the baseline model here. As the metal electrodes are made of highly thermally conductive materials, which can dissipate heat rapidly, there are additional considerations to ensuring accurate temperatures in the channel. As can be seen in Table 1, fixing the electrodes at standard room temperature can have significant impacts on flow. While the electrodes likely do not significantly conduct heat to bring the temperature to external

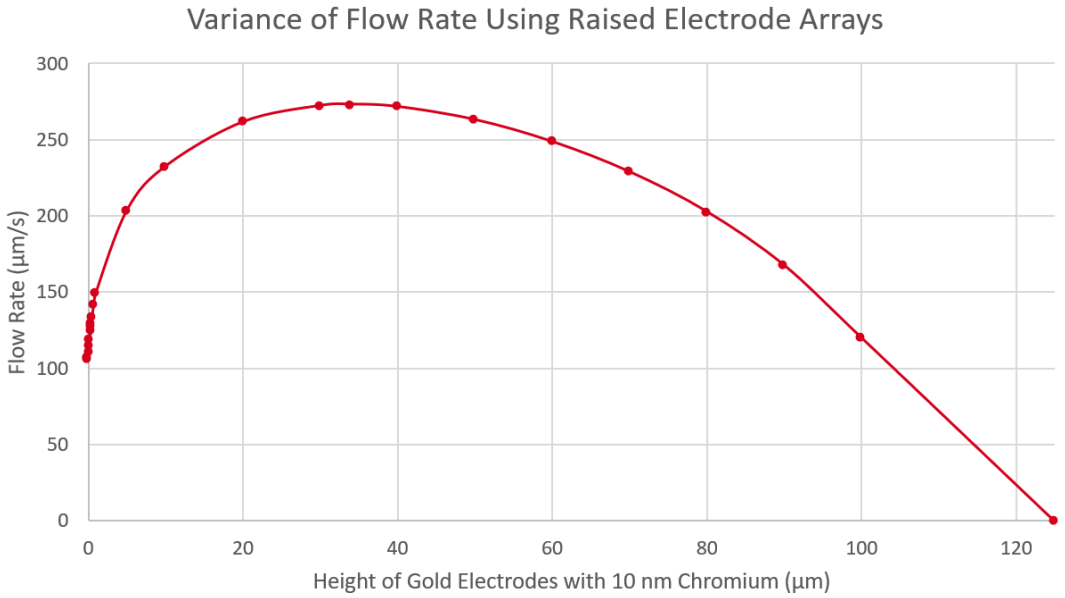

Figure 2: Graphical relationship showing the impacts of protrusion of electrodes into an ACET channel on outlet flow rate. Simulation uses a 300 um tall channel. Simulation bounds of electrode height for this relationship are not indicative of traditional fabrication methods, but used to outline the relationship at extremes.

conditions, the actual electrode temperature is likely to be lower than the COMSOL model predicts, which will lower expected temperature values, and thus flow. Additionally, modifying the viscosity term to include temperature dependent viscosity results in a significant positive change. Temperature dependent viscosity is a term that has been previously ignored in ACET work, but as can be seen in equation 5, is an important factor to consider. The equation used for temperature dependent viscosity can take several forms, but the one used in this work is seen in equation 9 [12]. The values in this equation are heavily dependent on material properties and will be unique to each individual media.

$$\eta = 2.414 \cdot 10^{-5} \cdot 10^{\frac{247.8}{T-140}} \tag{9}$$

Protrusion of electrodes, as noted in Table 1, plays a significant role in channel flow rates. Electrodes have been previously assumed to be of negligible height, flush with the surface, due to the significant discrepancies in average channel size compared to electrode thickness [2], [8], [17]. As such, simulations have been performed using a planar point source applied to the substrate to mimic an electrode. Table 1 shows that even extremely thin electrodes of dimensions typically used in sputtering fabrication can affect flow rates. Figure 2 shows the effects of increasing protrusion further into the channel. While distances on the order of tens of micrometers are unsuitable for microfabrication processes such as chemical or vapor deposition, standard PCB fabrication uses conductor thicknesses of approximately 17-35 µm. Line widths and relevant PCB material properties require further testing and validation, but this shows a possibility of the use of standard PCB fabrication methods to create custom ACET microchannels.

Dielectric coatings have been proposed as a method of improving ACET device efficiency, as higher voltages can be attained without risk of electrolysis occurring [16]. While the specific material parameters and functionality of dielectric coatings is not addressed in this paper, the impacts of dielectric Joule Heating are significant. Here a model is used with electrodes protruding into the solution by 120 nm and a conformal dielectric coating of thickness 100 nm and dielectric permittivity modelling that of titanium dioxide (ε_r' = 63.7, tan(δ) = 0.051) [19]. There was an observed 21.4% difference in flow rates when dielectric heating was incorporated, with the higher flow rate including heating. Dielectric heating is calculated as the product of the angular frequency, imaginary component of permittivity, and the norm of electric field. This may seem relevant to only dielectric coatings as traditional conductors have approximately zero loss tangent, however there is a marked increase in microfluidic technologies using organic polymers and novel electrode materials such as PEDOT-PSS, which can have large dielectric losses [20], [21].

Lastly, one key simplification used throughout ACET system modelling is the use of a two-dimensional model. Previous work stated a negligible difference between two and three dimensional simulations [2], [9] and this has been widely used throughout the field. The underlying concept for simplification is that channel width is typically several times larger than channel depth, and therefore the primary wall boundary that impacts flow is the channel base and top. There is, however, significant evidence, to show that flow conditions in microchannels are heavily affected by wall boundary conditions and channel shape, even with large ratios between width and depth [13], [22].The models initially used to state this were limited by computational power, the capability to make appropriately sized meshes, inability to assign appropriate boundary conditions, and limits on device scale that could be achieved. Given that computing systems have improved drastically, the relationship between a two- and three-dimensional equivalent system has been reassessed here. As can be seen in Figure 3, the effects of the no-slip boundary condition at the channel wall significantly impact the outlet flow rate.

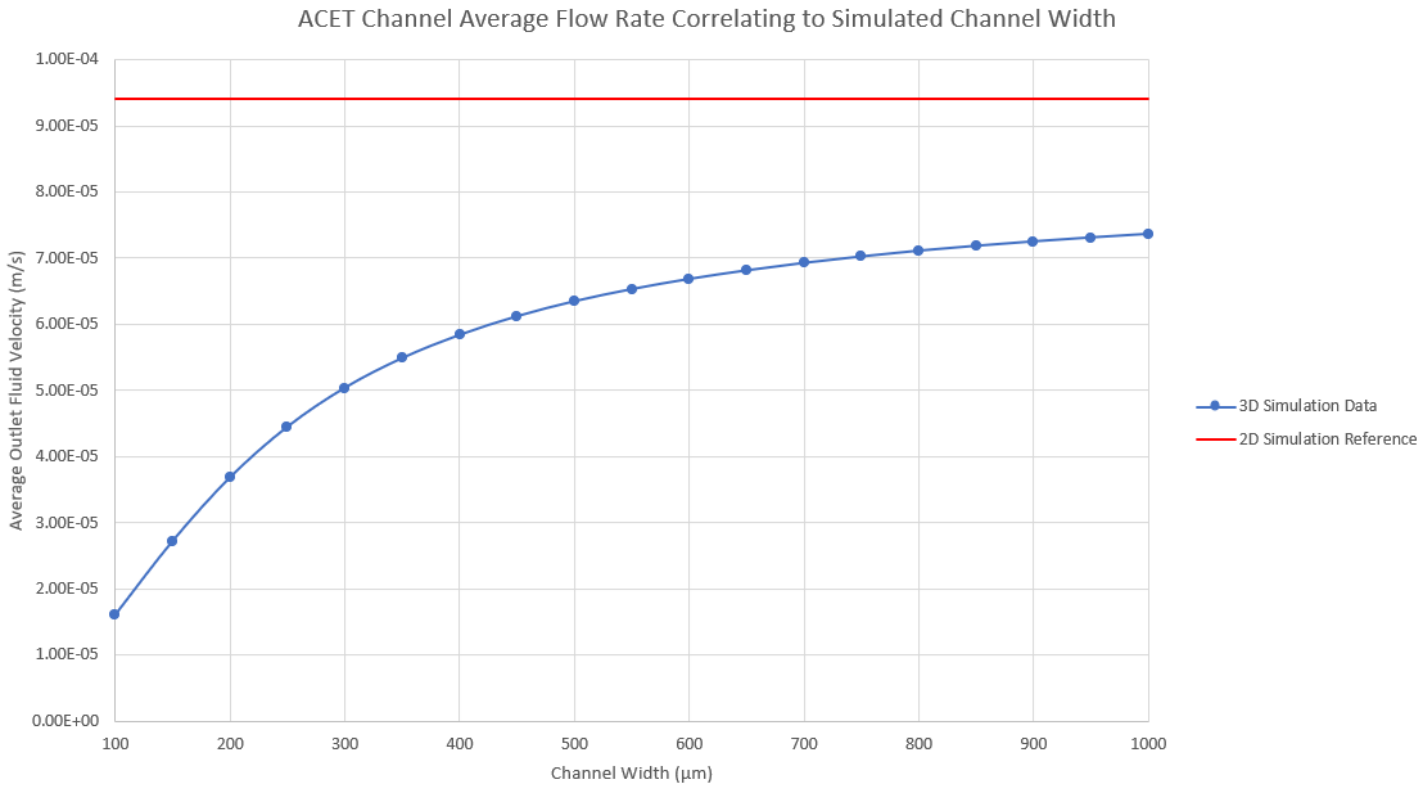

Figure 3: Relationship between simulated channel depth and outlet flow rates. In this case, depth means distance into the page (as seen in Figure 1), usually assumed to be negligible due to the high aspect ratio of microfluidic channels. Two dimensional reference value taken from simulations described in this work and used as a reference value in Table 1.

With a channel width:height ratio of 5:1 there was a 28% reduction in flow rate. This shows that using three-dimensional models is key in developing ACET simulations which accurately reflect real systems.

Conclusions

This work introduces several strategies and methods of pushing ACET simulations towards a more realistic model. Implementing simple changes previously thought to be negligible, such as convective cooling, electrode protrusion, and dielectric heating, are feasible methods of improving simulation accuracy. Other methods such as three-dimensional modelling are, expectedly, superior in developing a realistic ACET model compared to 2D. However these systems are still computationally intensive and may be unachievable by many researchers. Ultimately a three-dimensional model is still highly recommended. Certain parameters proposed here, such as no-slip conditions, temperature variable viscosity and electrode heat dissipation require further investigation, both experimentally and numerically to determine exact impacts.

Given increasing interest in electrokinetic techniques, and particularly ACET systems, for their applications in a wide variety of fields, developing accurate methods of simulating systems is key to the continual improvement and development of novel devices.

References

[1] Q. Lang *et al.*, "In-plane microvortices micromixer-based AC electrothermal for testing drug induced death of tumor cells," *Biomicrofluidics*, vol. 10, no. 6, p. 064102, Nov. 2016, doi: 10.1063/1.4967455.

[2] A. Salari, M. Navi, T. Lijnse, and C. Dalton, "AC Electrothermal Effect in Microfluidics: A Review," *Micromachines*, vol. 10, no. 11, p. 762, Nov. 2019, doi: 10.3390/mi10110762.

[3] G. Kunti, J. Dhar, A. Bhattacharya, and S. Chakraborty, "Alternating Current Electrothermal Flow for Energy Efficient Thermal Management of Microprocessor Hot Spots," in *2019 25th International Workshop on Thermal Investigations of ICs and Systems (THERMINIC)*, Sep. 2019, pp. 1–6, doi: 10.1109/THERMINIC.2019.8923474.

[4] R. H. Vafaie, H. B. Ghavifekr, H. V. Lintel, J. Brugger, and P. Renaud, "Bi-directional ACET micropump for on-chip biological applications," *ELECTROPHORESIS*, vol. 37, no. 5–6, pp. 719–726, 2016, doi: 10.1002/elps.201500404.

[5] A. Salari and C. Dalton, "Fast Biofluid Transport of High Conductive Liquids Using AC Electrothermal Phenomenon, A Study on Substrate Characteristics," Oct. 2014, doi: 10.13140/2.1.2183.0085.

[6] T. Lijnse, S. Cenaiko, and C. Dalton, "Prevention of Electrode Degradation in ACET Micropumps for Biomedical Devices," presented at the Alberta Biomedical Engineering Conference, Banff, Canada, Oct. 2019.

[7] Q. Yuan, K. Yang, and J. Wu, "Optimization of planar interdigitated microelectrode array for biofluid transport by AC electrothermal effect," *Microfluid. Nanofluidics*, vol. 16, no. 1, pp. 167–178, Jan. 2014, doi: 10.1007/s10404-013-1231-8.

[8] E. Du and S. Manoochehri, “Optimal design of microgrooved channels with electrokinetic pumping for lab-on-achip applications,” *IET Nanobiotechnol.*, vol. 4, no. 2, pp. 40–49, Jun. 2010, doi: 10.1049/iet-nbt.2009.0015.
[9] M. Lian and J. Wu, “Ultrafast micropumping by biased alternating current electrokinetics,” *Appl. Phys. Lett.*, vol. 94, no. 6, p. 064101, Feb. 2009, doi: 10.1063/1.3080681.
[10] N. G. Green, A. Ramos, A. González, H. Morgan, and A. Castellanos, “Fluid flow induced by nonuniform ac electric fields in electrolytes on microelectrodes. I. Experimental measurements,” *Phys. Rev. E*, vol. 61, no. 4, pp. 4011–4018, Apr. 2000, doi: 10.1103/PhysRevE.61.4011.
[11] A. Ramos, H. Morgan, N. G. Green, and A. Castellanos, “Ac electrokinetics: a review of forces in microelectrode structures,” *J. Phys. Appl. Phys.*, vol. 31, no. 18, pp. 2338–2353, Sep. 1998, doi: 10.1088/0022-3727/31/18/021.
[12] A. Salari, M. Navi, and C. Dalton, “A novel alternating current multiple array electrothermal micropump for lab-on-a-chip applications,” *Biomicrofluidics*, vol. 9, no. 1, Feb. 2015, doi: 10.1063/1.4907673.
[13] G. E. Karniadakis, A. Beskok, and N. Aluru, *Microflows and Nanoflows: Fundamentals and Simulation*. New York: Springer-Verlag, 2005.
[14] M. R. Hossan, D. Dutta, N. Islam, and P. Dutta, “Review: Electric field driven pumping in microfluidic device,” *Electrophoresis*, vol. 39, no. 5–6, pp. 702–731, 2018, doi: 10.1002/elps.201700375.
[15] H. Morgan and N. G. Green, “AC ELECTROKINETICS: COLLOIDS AND NANOPARTICLES.,” 2002.
[16] T. Lijnse, S. Cenaiko, and C. Dalton, “Numerical simulation of a tuneable reversible flow design for practical ACET devices,” *SN Appl. Sci.*, vol. 2, no. 2, p. 305, Jan. 2020, doi: 10.1007/s42452-020-2098-4.
[17] F. J. Hong, F. Bai, and P. Cheng, “Numerical simulation of AC electrothermal micropump using a fully coupled model,” *Microfluid. Nanofluidics*, vol. 13, no. 3, pp. 411–420, Sep. 2012, doi: 10.1007/s10404-012-0965-z.
[18] J. C. T. Eijkel, C. Dalton, C. J. Hayden, J. P. H. Burt, and A. Manz, “A circular ac magnetohydrodynamic micropump for chromatographic applications,” *Sens. Actuators B Chem.*, vol. 92, no. 1, pp. 215–221, Jul. 2003, doi: 10.1016/S0925-4005(03)00267-3.
[19] A. Wypych *et al.*, “Dielectric Properties and Characterisation of Titanium Dioxide Obtained by Different Chemistry Methods,” *Journal of Nanomaterials*, Mar. 19, 2014. https://www.hindawi.com/journals/jnm/2014/124814/ (accessed Sep. 10, 2020).
[20] V. Yuste-Sanchez, F. Gonzalez-Gonzalez, M. Hoyos, M. A. López Manchado, and R. Verdejo, “Dielectric Properties of All-Organic Coatings: Comparison of PEDOT and PANI in Epoxy Matrices,” *J. Compos. Sci.*, vol. 4, no. 1, Art. no. 1, Mar. 2020, doi: 10.3390/jcs4010026.
[21] T. Chen *et al.*, “Ultra high permittivity and significantly enhanced electric field induced strain in PEDOT:PSS–RGO@PU intelligent shape-changing electro-active polymers,” *RSC Adv.*, vol. 4, no. 109, pp. 64061–64067, Nov. 2014, doi: 10.1039/C4RA10695D.
[22] J. M. MacInnes, X. Du, and R. W. K. Allen, “Prediction of electrokinetic and pressure flow in a microchannel T-junction,” *Phys. Fluids*, vol. 15, no. 7, pp. 1992–2005, Jun. 2003, doi: 10.1063/1.1580479.

Acknowledgements

The authors would like to acknowledge the Natural Sciences and Engineering Research Council of Canada and Alberta Innovates for support of this work. Additionally, the authors thank CMC Microsystems for provision of software.